Linking crenarchaeal and bacterial nitrification to anammox in the Black Sea

Phyllis Lam*†, Marlene M. Jensen‡, Gaute Lavik*, Daniel F. McGinnis§, Beat Müller§, Carsten J. Schubert§, Rudolf Amann*, Bo Thamdrup‡, and Marcel M. M. Kuypers*

*Max Planck Institute for Marine Microbiology, Celsiusstrasse 1, 28359 Bremen, Germany; ‡Nordic Center for Earth Evolution, Institute of Biology, University of Southern Denmark, Campusvej 55, 5230 Odense M, Denmark; and §Surface Waters-Research and Management, Swiss Federal Institute of Aquatic Science and Technology (EAWAG), Seestrasse 79, CH-6047 Kastanienbaum, Switzerland

Edited by David M. Karl, University of Hawaii, Honolulu, HI, and approved March 1, 2007 (received for review December 15, 2006)

Active expression of putative ammonia monooxygenase gene subunit A (*amoA*) of marine group I *Crenarchaeota* has been detected in the Black Sea water column. It reached its maximum, as quantified by reverse-transcription quantitative PCR, exactly at the nitrate maximum or the nitrification zone modeled in the lower oxic zone. Crenarchaeal *amoA* expression could explain 74.5% of the nitrite variations in the lower oxic zone. In comparison, *amoA* expression by γ-proteobacterial ammonia-oxidizing bacteria (AOB) showed two distinct maxima, one in the modeled nitrification zone and one in the suboxic zone. Neither the *amoA* expression by crenarchaea nor that by β-proteobacterial AOB was significantly elevated in this latter zone. Nitrification in the suboxic zone, most likely microaerobic in nature, was verified by $^{15}NO_2^-$ and $^{15}N^{15}N$ production in $^{15}NH_4^+$ incubations with no measurable oxygen. It provided a direct local source of nitrite for anammox in the suboxic zone. Both ammonia-oxidizing crenarchaea and γ-proteobacterial AOB were important nitrifiers in the Black Sea and were likely coupled to anammox in indirect and direct manners respectively. Each process supplied about half of the nitrite required by anammox, based on ^{15}N-incubation experiments and modeled calculations. Because anammox is a major nitrogen loss in marine suboxic waters, such nitrification–anammox coupling potentially occurring also in oceanic oxygen minimum zones would act as a short circuit connecting regenerated ammonium to direct nitrogen loss, thus reducing the presumed direct contribution from deep-sea nitrate.

ammonia-oxidizing bacteria | *amoA* gene expression | marine group | *Crenarchaeota* | marine nitrogen loss

Nitrification, the stepwise oxidation of ammonium to nitrite and then nitrate, is a key process in marine nitrogen cycling. It is responsible for the formation of the large deep-sea nitrate reservoir. It connects the recycling of organic nitrogen to the ultimate nitrogen loss from the oceans, because its products are substrates for denitrification and anaerobic ammonium oxidation (anammox), the only two presently known nitrogen loss processes. In productive waters such as upwelling regions, high fluxes of organic matter and thus remineralization create strong subsurface oxygen minima, enabling denitrification (1–4) or anammox (5–8) to occur. Nitrogen losses from these oxygen minimum zones (OMZs) are estimated to account for 30–50% of total nitrogen loss from the oceans (9, 10). Because remineralization also releases large amounts of ammonium, high nitrification rates are often associated with these OMZs (11), implying that nitrification may play an important role in promoting marine nitrogen loss.

The Black Sea is the largest marine anoxic basin in the world. A 20- to 40-m-thick suboxic transitional zone, characterized by low oxygen (<5 μM) and undetectable sulfide, persists throughout the basin between the surface oxic layer and the sulfidic anoxic deep water (≥100 m) (12, 13). The exact depth zonation varies according to the location within the basin because of circulation and gyre formation, but similar concentrations of chemical species can be traced along isopycnals or density (σ_t) surfaces throughout the basin (12). Therefore, the Black Sea provides an ideal model system to study nitrogen cycling processes along oxygen gradients. Nitrification has been reported in the lower oxic zone (14) and so has nitrogen loss via anammox in the suboxic zone (15). Nevertheless, the identity and abundance of the responsible nitrifiers, or any coupling between nitrification and nitrogen losses, remain poorly documented.

The first and rate-limiting step of nitrification is aerobic ammonia oxidation. It is a microbially mediated reaction. For decades, only specific groups of β- and γ-proteobacteria have been found to exhibit this capability. However, recent metagenomic studies in the Sargasso Sea (16, 17) and later of a marine sponge symbiont (18) have identified in marine group I (MGI) *Crenarchaeota* genes encoding proteins resembling ammonia monooxygenase (AMO), the key enzyme in aerobic ammonia-oxidizing bacteria (AOB). This chemoautotrophic ammonia-oxidizing potential was confirmed in *Candidatus* "Nitrosopumilus maritimus," an MGI crenarchaeon isolated from a marine aquarium (19). This crenarchaeon is highly similar to the Sargasso Sea phylotypes based on their 16S rRNA (>98% sequence identity) and putative AMO (93–98% amino acids homology) sequences. This putative AMO is, however, only 38–51% (amino acids) homologous to those of AOB. Since then, similar sequences of crenarchaeal AMO gene subunit A (*amoA*) (69–99% amino acid homology) have been detected in various marine water columns and sediments, including the Black Sea (20). Because nonthermophilic MGI *Crenarchaeota* constitute a significant portion of oceanic picoplankton (up to 30%) (21, 22) and a considerable fraction are likely autotrophic (23, 24), it is speculated that these MGI *Crenarchaeota* could be more important nitrifiers in the oceans than the usually less abundant AOB (18, 19). Indeed, crenarchaeal *amoA* genes were reported to be more abundant than bacterial *amoA* in a North Atlantic study (25). However, no published data to date have shown crenarchaeal *amoA* expression in marine environments.

In this study, we provide direct evidence of crenarchaeal *amoA* activities in the Black Sea water column. Its expression was com-

Author contributions: P.L., M.M.J., B.T., and M.M.M.K. designed research; P.L., M.M.J., G.L., D.F.M., B.T., and M.M.M.K. performed research; D.F.M., B.M., C.J.S., and R.A. contributed new reagents/analytical tools; P.L., M.M.J., G.L., B.T., and M.M.M.K. analyzed data; and P.L. and M.M.M.K. wrote the paper.

The authors declare no conflict of interest.

This article is a PNAS Direct Submission.

Freely available online through the PNAS open access option.

Abbreviations: AOB, ammonia-oxidizing bacteria; βAOB, β-proteobacterial AOB; γAOB, γ-proteobacterial AOB; MGI, marine group I; *amoA*, ammonia monooxygenase gene subunit A; OMZ, oxygen minimum zone; AMO, ammonia monooxygenase; CARD, catalyzed reporter deposition; qPCR, quantitative PCR; OTU, operational taxonomic unit.

Data deposition: The sequences reported in this paper have been deposited in the GenBank database (accession nos. EF414229–EF414283).

See Commentary on page 6881.

†To whom correspondence should be addressed. E-mail: plam@mpi-bremen.de.

This article contains supporting information online at www.pnas.org/cgi/content/full/0611081104/DC1.

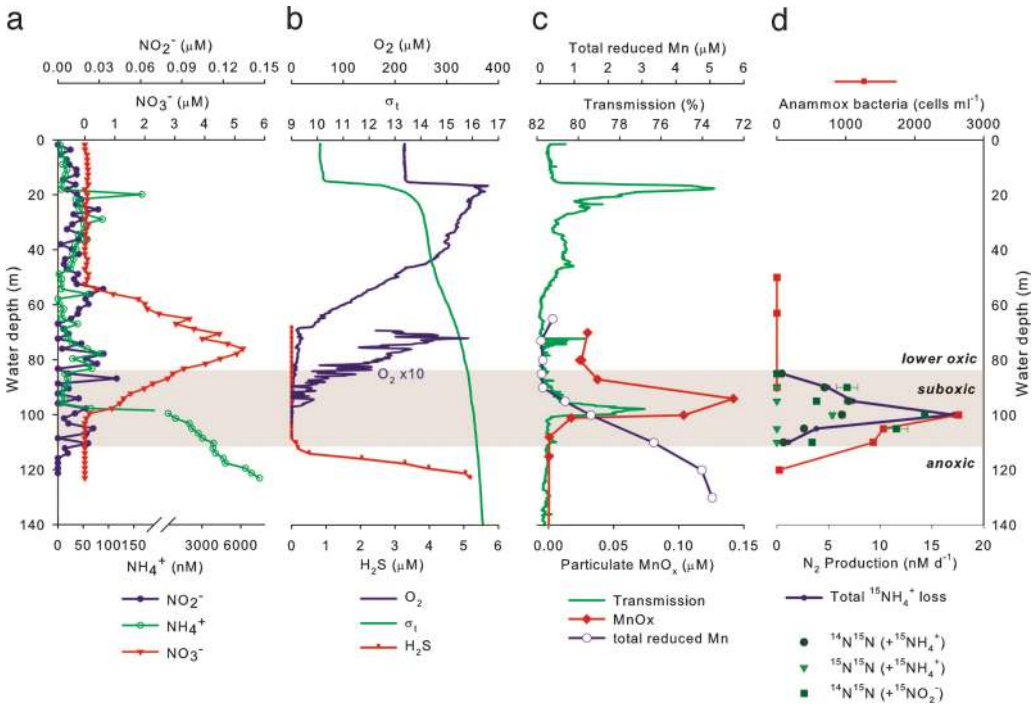

Fig. 1. Vertical distribution of inorganic nitrogen (*a*), O_2 and sulfide (*b*), light transmission, particulate MnO_x, and total reduced Mn (*c*), and anammox bacterial abundance and $^{15}N_2$ production rates (*d*).

pared quantitatively with that of bacterial *amoA*. In addition, coupling between nitrification and anammox was examined by using a combination of gene abundance and expression analyses, high-resolution chemical profiling, reaction-diffusion modeling, and ^{15}N incubation experiments.

Results and Discussion

Hydrochemical Settings. In accord with previous findings, dissolved oxygen in the central Black Sea (43°14.9′N, 34°00.0′E) [supporting information (SI) Fig. 5] decreased from fully oxic to <5 μM at 85 m (σ_t = 15.83, for comparison with studies in other parts of the basin) (Fig. 1). The suboxic zone extended from this depth to 112 m (σ_t = 16.15) below which sulfide started to accumulate. Nitrate formed a distinct maximum (≈5 μM) centered ≈76 m (σ_t = 15.61), but dropped to background or below detection shallower than 55 m or deeper than 100 m. Nitrite was slightly elevated (20–42 nM) at ≈55, 80 and 105 m, and was otherwise close to detection limit. Ammonium levels were <80 nM in the oxic zone except for slight elevations at 20 m and 78 m, and increased substantially upon nitrate disappearance to micromolar levels below 100 m. From the NO_x^- concentration profile, a reaction-diffusion model was used to calculate total net NO_x^- production rates of up to 10 nM day^{-1} at 78 m (Fig. 2*d*), which were within the range of the potential nitrification rates (5–50 nM day^{-1}) previously measured (14). Our model showed that net nitrification occurred only within a narrow zone (71–81 m) (Fig. 2).

Active Microbial Community Structure. Bacteria (38–60% of total microbial abundance as DAPI-stained cells) dominated over Archaea (5–20% DAPI) in all sampled depths based on 16S rRNA-targeted catalyzed reporter deposition (CARD)-FISH results (SI Fig. 6). The highest bacterial abundance and 16S rRNA transcript levels [measured by reverse-transcription quantitative PCR (qPCR)] were reached at the nitrate maximum and the oxic–anoxic interface, coinciding with elevated dark CO_2 fixation rates (SI Fig. 6). The archaeal populations were largely *Crenarchaeota* (41–95% of total Archaea), whose contribution to the total community peaked at the nitrification zone (19% DAPI). Active archaeal communities at 80 m, 100 m, and 105 m comprised exclusively of MGI *Crenarchaeota*, as revealed by phylogenetic analyses of reverse-transcribed 16S rRNA. The majority shares 92–99% sequence identity with the ammonia-oxidizing isolate *Candidatus*"*N. maritimus*", and belong to the large MGI α-cluster (SI Fig. 7). Sequences retrieved from different depths did not form disparate subclusters. Anammox bacteria were present only in the suboxic zone, as verified by CARD-FISH and quantified by qPCR of their 16S rRNA genes, reaching a maximum at 100 m (2.6×10^3 cells ml^{-1}) where the highest anammox rate was measured (M.M.J., B.T., G.L., and M.M.M.K., unpublished results) (Fig. 1). The highest γ-proteobacterial AOB abundance (5.4×10^3 cells ml^{-1}) was also observed at this depth (Fig. 2).

Active Expression of Crenarchaeal Putative *amoA* Genes. Crenarchaeal putative *amoA* was strongly expressed within the narrow nitrification zone, whereas close to background levels were measured at other depths (Fig. 2). In comparison, high gene abundance was also observed near the oxic–anoxic interface, where there were secondary maxima in crenarchaeal cellular and 16S rRNA transcript abundance. The identities of crenarchaeal *amoA* genes were confirmed by clone library screening at both DNA and mRNA levels at 80 m, 100 m, and 110 m, representing the lower oxic, suboxic zones, and oxic–anoxic interface, respectively. The sequences retrieved are 70–91% homologous to the *amoA* of *Candidatus* "N. maritimus" at the nucleotide level, but only 33–37% and 30–37% to those of β- and γ-proteobacterial ammonia-oxidizing bacteria (βAOB and γAOB), respectively. Eleven operational taxonomic units (OTUs) were identified in total, with three unique to 80 m (BS157-G8/-D4/-H3) and two to 100 m (BS160-F11/-G4). More diverse crenarchaeal *amoA* were expressed in the nitrification zone compared with the two deeper depths (Fig. 3). Most of the obtained sequences fell into the marine clusters A, B, and C (20), but three OTUs fell into the "sediment" cluster, which also included *Candidatus* "N. maritimus."

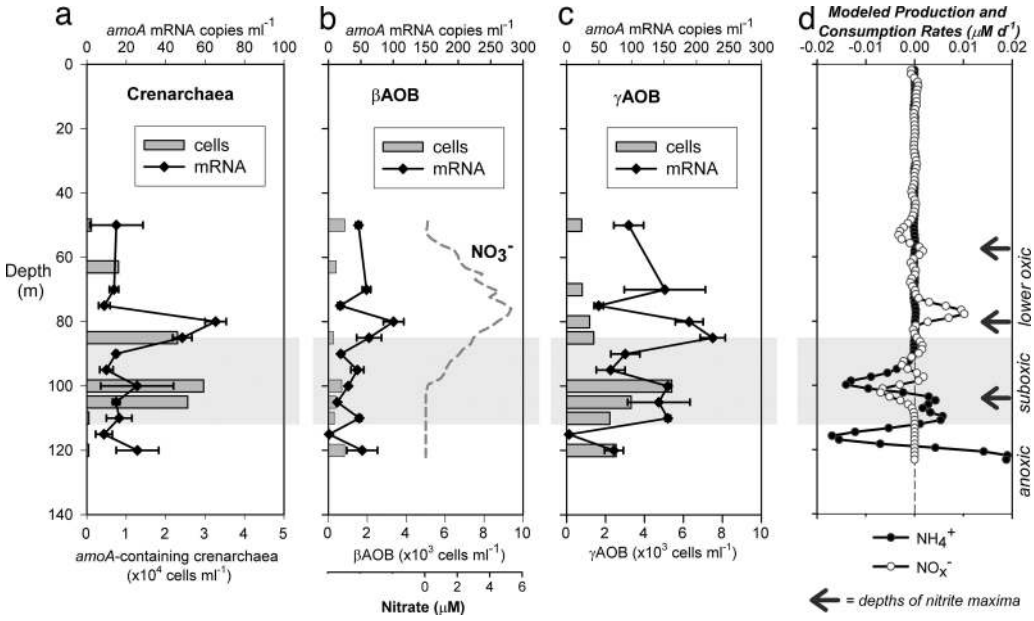

Fig. 2. Vertical distribution of *amoA* expression (mean ± SD from 3× qPCR) by, and cellular abundance of: putative ammonia-oxidizing crenarchaea (*a*), βAOB (*b*), and γAOB (*c*). Abundance of putative ammonia-oxidizing crenarchaea was estimated as crenarchaeal CARD-FISH cell counts multiplied by *amoA*:16S rRNA gene ratios (except for 100 m and 105 m where ratio was >1, crenarchaeal CARD-FISH counts were used directly). γAOB were direct CARD-FISH counts, and βAOB abundance was estimated as βAOB:γAOB *amoA* gene copy ratios × γAOB cell counts ÷ 3 [typical *amoA* gene copies in βAOB (59)]. (*d*) Modeled production and consumption rates of NH_4^+ and NO_x^-.

Crenarchaeal Versus Bacterial Ammonia Oxidation in the Lower Oxic Zone. Despite the barely detectable gene abundance, strong *amoA* expression by AOB was detected within the nitrification zone (Fig. 2). γAOB *amoA* expression, in particular, was up to nearly 3-fold greater than that of crenarchaea. If we assume AOB cellular nitrification rates of 6–20 fmol of N cell^{-1} day^{-1} (26, 27), the abundance of AOB (≤1,400 cells ml^{-1}) present might support at most a rate of 7–24 nM day^{-1}. Although this rate estimate lies in the same range as the modeled net nitrification rate (10 nM day^{-1}), it is insufficient to meet the upper range of 5–50 nM day^{-1} previously measured (14). Some other organisms had to be nitrifying at the same time, and would most likely be the highly abundant MGI *Crenarchaeota* (4.3×10^4 cells ml^{-1}).

The striking correspondence of the maximum crenarchaeal *amoA* gene expression and gene abundance, to the NO_x^- maxima and the narrow modeled nitrification zone, indicates that MGI *Crenarchaeota* were involved in nitrification in the lower oxic zone. Compared with total AOB *amoA*, crenarchaeal *amoA* genes were 43-fold more abundant (SI Table 1). This crenarchaeal *amoA* predominance is consistent with the observations in the two environmental studies that compared crenarchaeal and bacterial ammonia-oxidizers (25, 28). If we assume a crenarchaeal cellular nitrification rate of 2–4 fmol of N cell^{-1} day^{-1} (25) and that each crenarchaeal cell contains at most one copy of *amoA* gene, based on the metagenome of *Cenarchaeum symbiosum* (18), *amoA*-containing crenarchaea in the nitrification zone (2.3×10^4 cells ml^{-1}) could account for an NO_x^- production of 46–92 nM day^{-1}. The lower end of this estimate would have already been sufficient to explain the previously measured rate (5–50 nM day^{-1}) (14) and exceeds our modeled rate (10 nM day^{-1}).

Whereas an increase in *amoA* mRNA levels within the same group of organisms might indicate their respective elevated nitrification rates, as suggested in some transcription studies with AOB (29–32) and a soil crenarchaeon (33) upon NH_4^+ stimuli, the absolute quantities of *amoA* mRNA should not be singularly used to compare nitrifying activities amongst different groups. This is because transcriptional regulation involves a complex network of global and specific regulators that the amount of *amoA* mRNA transcribed per mole of NH_3 oxidized would almost certainly vary amongst species, physiological states or environmental conditions. Different species might possess different numbers of *amoA* gene copies per cell, such as the variations in crenarchaeal *amoA*:16S rRNA gene ratios observed in the Black Sea water column (oxic, 0.3–0.7; suboxic, 1.2–2.8; anoxic, 0.01–0.04) (SI Table 1) or in the North Atlantic study (25), although the possibility of other unknown organisms possessing *amoA*-like genes such as in the suboxic zone cannot be ruled out either. In addition, the stability and maintenance levels of *amoA* mRNA might differ from one group to another. At least some AOB are known to maintain low *amoA* mRNA levels even after prolonged starvation (29). It is possible that AOB in the Black Sea maintained a higher background *amoA* mRNA level than their crenarchaeal counterparts, and so a consistently higher bacterial *amoA* mRNA level despite low cell abundance. Besides, the gene encoding hydroxylamine oxidoreductase (*hao*), the enzyme responsible for the final energy-yielding step of ammonia oxidation, has not been identified in the metagenome of *C. symbiosum* (18). Considering also the different organization of *amo* subunits in a crenarchaeal genome versus AOBs (17, 18), ammonia-oxidizing crenarchaea may have an alternative energy-yielding system. Their *amoA* mRNA synthesis and degradation rates are not necessarily the same.

By using a statistical approach, a multiple stepwise linear regression demonstrated that within the lower oxic zone, crenarchaeal and γAOB *amoA* mRNA were the only valid predictors (out of the variables measured in this study) for nitrite distributions ($r^2 = 0.81$, $P < 0.05$), the direct product of ammonia oxidation. Crenarchaeal *amoA* mRNA variation can explain 74.5% of the nitrite variation within the oxic zone, whereas γAOB *amoA* mRNA only accounts for 6.5%. This statistical analysis suggests that nitrite distribution and therefore nitrification in this zone was mainly controlled by crenarchaeal *amoA* expression.

Direct Nitrification–Anammox Coupling in the Suboxic Zone. Since the first discovery of anammox in marine water columns (15, 34), where

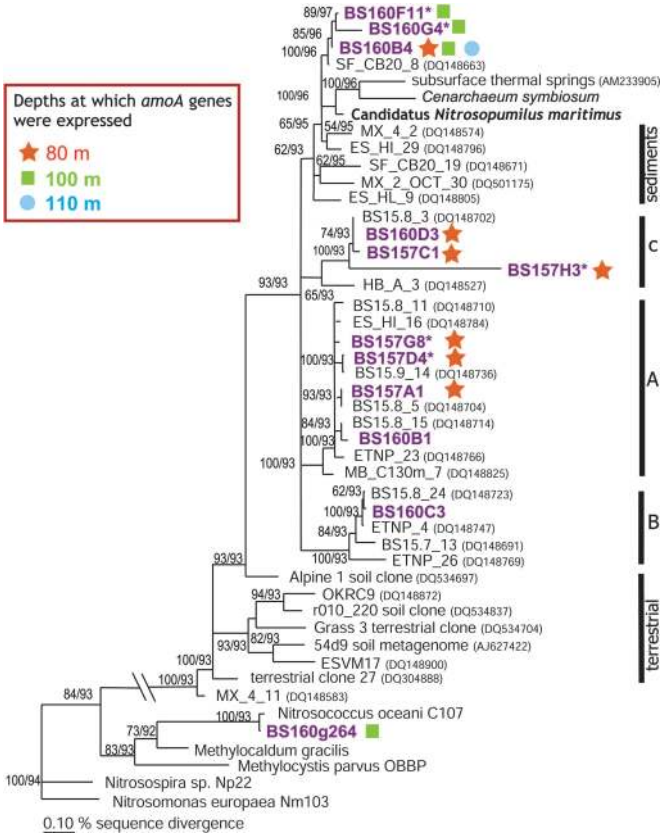

Fig. 3. A maximum likelihood tree of bacterial and crenarchaeal *amoA* obtained in the Black Sea water column. Branching patterns are supported by >50% bootstrap values (1,000×) by means of maximum parsimony and distance methods, and their respective %bootstrap values are denoted. Only representative OTUs (<98% sequence identity) are shown (in bold). An OTU marked with an asterisk indicates its uniqueness to that depth. The marine A, B, and C and sediment clusters previously defined (20) are also shown. The symbols (stars, squares, circles) indicate expressed sequences.

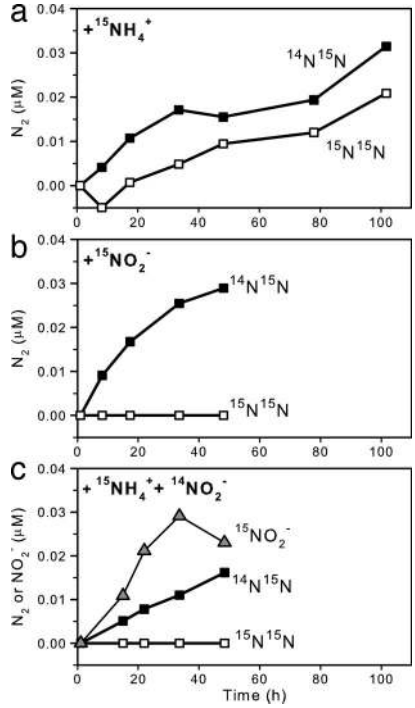

Fig. 4. ^{15}N-incubation experiments with production of $^{14}N^{15}N$ and $^{15}N^{15}N$ from $^{15}NH_4^+$ (*a*), $^{14}N^{15}N$ and $^{15}N^{15}N$ from $^{15}NO_2^-$ (*b*), and $^{14}N^{15}N$, $^{15}N^{15}N$, and $^{15}NO_2^-$ from $^{15}NH_4^+ + {}^{14}NO_2^-$ (*c*).

NH_4^+ and NO_2^- combine to produce gaseous N_2, it has been an enigma whether NO_2^- comes from nitrification or nitrate reduction or both. Anammox occurred in the Black Sea suboxic zone and peaked at 100 m (≈11 nmol of N_2 liter^{-1} day^{-1}), where NO_3^- and NH_4^+ profiles intersected (Fig. 1) (M.M.J., B.T., G.L., and M.M.M.K., unpublished results). The reaction-diffusion model revealed a narrow zone (90–102 m) of net NH_4^+ loss reaching 14.1 nM day^{-1} at 100 m, or an integrated rate of 75.2 μmol of N m^{-2} day^{-1} (Fig. 2*d*). This NH_4^+ loss is double the total net NO_x^- consumption rate around these depths (≤ 7.0 nM day^{-1} or 36.7 μmol of N m^{-2} day^{-1}). The total NO_x^- production in the oxic zone (55.5 μmol of N m^{-2} day^{-1}) also could not match this NH_4^+ loss because of anammox, which consumes 1 mol of NO_2^- per mol of NH_4^+ oxidized. Therefore, an additional local source of NO_2^- and/or an additional loss of NH_4^+ must be present to reconcile the difference.

The best candidate to explain this phenomenon is microaerobic or anaerobic nitrification, whose direct coupling with anammox, the so-called completely autotrophic nitrogen removal over nitrite (CANON), has been demonstrated in bioreactors (35, 36). At 100 m, nitrification was evidenced by the production of $^{15}NO_2^-$ (12.9 nM day^{-1}) in incubations with $^{15}NH_4^+ + {}^{14}NO_2^-$ and no measurable oxygen (Fig. 4). Parallel incubations with the addition of allylthiourea, an inhibitor specific for aerobic ammonia oxidation, yielded no $^{15}NO_2^-$ production. Exposure to 5 μM of oxygen almost doubled the $^{15}NO_2^-$ production rate (25.8 nM day^{-1}) and previous oxic incubations have measured rates of ≈82 nM day^{-1} (14), thus supporting the presence and activities of the normally aerobic ammonia-oxidizers. Furthermore, coupling with anammox was directly shown in anammox rate measurements (M.M.J., B.T., G.L., and M.M.M.K., unpublished results) based on isotope pairing. Because of the 1-to-1 NH_4^+:NO_2^- stoichiometry and the fact that only one of these nitrogen pools was labeled with ^{15}N at a time, anammox should produce $^{15}N^{14}N$ (and $^{14}N^{14}N$) in all ^{15}N incubations, and denitrification should produce $^{15}N^{15}N$, $^{15}N^{14}N$ (and $^{14}N^{14}N$) in $^{15}NO_2^-$ incubations. Surprisingly, N_2 gas in the form of $^{15}N^{15}N$ (4.6 ± 0.7 nmol of N_2 liter^{-1} day^{-1}) was produced at similar rates as $^{15}N^{14}N$ (6.8 ± 1.0 nmol of N_2 liter^{-1} day^{-1}) in incubations with $^{15}NH_4^+$ alone; but no $^{15}N^{15}N$ was produced in incubations with $^{15}NO_2^-$ or $^{15}NH_4^+ + {}^{14}NO_2^-$ (Figs. 1 and 4). Clearly, the production of $^{15}N^{15}N$ in $^{15}NH_4^+$ incubations was a result of anammox being linked to nitrifiers when no other NO_2^- was readily available for anammox, whereas the lack of $^{15}N^{15}N$ produced in $^{15}NO_2^-$ incubations indicates the absence of denitrification. In other words, both the modeled fluxes and ^{15}N-incubations indicate that the NO_2^- flux from the lower oxic zone could only fuel about half of the total anammox N_2 production, whereas the rest of NO_2^- likely came from *in situ* nitrification. Consequently, the total NH_4^+ loss because of direct nitrification-anammox coupling and regular anammox (2 × $^{15}N^{15}N$ and 1 × $^{14}N^{15}N$ production, because the NH_4^+ pool was essentially all ^{15}N) would amount to ≈17 nM day^{-1} at 100 m, which is in good agreement with our modeled net NH_4^+ consumption (14.1 nM day^{-1}). In addition, if the excess modeled net NH_4^+ loss over net NO_x^- loss (i.e., 14.1 − 7.0 = 7.1 nM day^{-1}) was totally channeled to direct nitrification-anammox coupling, in which half of the NH_4^+ was taken up directly by anammox and the rest indirectly as NO_2^- after nitrification, then a total anammox rate as N_2 production would be: 7.0 + (7.1 ÷ 2) = 10.55 nmol of N_2 liter^{-1} day^{-1}. This estimate is essentially the same as the rate measured by isotope-pairing (11.1 ± 1.7 nmol of N_2 liter^{-1} day^{-1}) (M.M.J., B.T., G.L., and M.M.M.K., unpublished results).

Further evidence of nitrification at 100 m is provided by the

strong expression of γAOB *amoA*, which formed a distinct secondary maximum, along with their highest cell abundance (5.4×10^3 cells ml^{-1}). The identity of this expressed γAOB *amoA* was verified by a clone library constructed for this depth, retrieving sequences of 97% nucleotide sequence identity as *Nitrosococcus oceani* (Fig. 3). γAOB *amoA* expression was consistent with the inhibition of $^{15}NO_2^-$-production by allylthiourea. Assuming a cellular nitrification rate of 6–20 fmol of N $cell^{-1}$ day^{-1}, these γAOB might potentially support nitrification rates of 32–108 nM day^{-1}, or 328–1,094 μmol of N m^{-2} day^{-1} integrated over 98–113 m, which is in the same order as the integrated anammox rates (293–406 μmol of N m^{-2} day^{-1}) over the suboxic zone (M.M.J., B.T., G.L., and M.M.M.K., unpublished results). The cooccurrence of AOB and anammox bacteria at this depth was also reflected in their correlated abundances (Kendall $\tau = 0.62$, $P < 0.05$ for βAOB and Pearson-correlation $R = 0.86$, $P < 0.05$ for γAOB), as well as their clustering in a principal component analysis (see *SI Appendix*).

The occurrence of nitrification in the absence of measurable oxygen is intriguing. By using a free-falling CTD equipped with an oxygen sensor (detection range 0–120% saturation, accuracy 2% sat.), we observed considerable temporal fluctuations in oxygen in the suboxic layer within a day (SI Fig. 8). These fluctuations were most likely lateral intrusions of oxygenated water, as the injections of foreign waters with different physical properties were evident from the deviations in temperature-salinity signatures and particle concentrations (% transmission) (SI Fig. 8). Whether these trace lateral oxygen intrusions were remnants of shelf-mixing brought in by the fringe of the Rim Current (37), or fossil turbulence from past local instabilities (38) or lateral intrusions of the Bosporus plume (39) reaching this far, remains to be determined. Despite a usual preference for oxic conditions by AOB, because of NH_4^+ availability AOB are often found actively nitrifying near oceanic OMZs (2, 3, 26), or even in virtually anoxic conditions (40, 41). At least some communities have shown low-oxygen adaptations by having a much higher oxygen affinity than their counterparts inhabiting high-oxygen settings (42). Although O_2 was hardly detectable at 100 m, the amount of nitrification occurring at this depth required only nanomolar levels of O_2, which is far below the detection limits of the instrumentation or chemical analyses currently available (≈1.5–2 μM). Alternatively, Mn(III)/(IV) may potentially serve as electron acceptors for anaerobic nitrification (43, 44), and they were detected as particulate MnO_x right around this depth (Fig. 1). Nonetheless, as the oxidation of dissolved Mn(II)/(III) diffusing from below required oxygen, the presence of the oxidative product particulate MnO_x itself at this depth indicated the presence of oxygen. Because nitrification with oxygen is thermodynamically more favorable than with MnO_2 ($\Delta G_{R\ pH\ =\ 7} = -341$ kJ mol^{-1} versus -175 kJ mol^{-1}) (44), the former reaction would expectedly be preferred when both electron acceptors are present.

Despite their high abundance and metabolic activities (revealed by 16S rRNA levels) of the potentially ammonia-oxidizing crenarchaea, their putative *amoA* genes were not expressed at significantly elevated levels in the Black Sea suboxic zone. These observations may imply that in such suboxic settings, these crenarchaea were not using their nitrifying capabilities much but some other energy-acquisition pathways. For instance, MGI *Crenarchaeota* have been shown to take up amino acids in the North Atlantic, and the proportion of organotrophy, as reflected by the uptake ratio of D- to L-amino acids, increased with depth in the meso- and bathypelagic realms (45). In contrast, the significantly enhanced *amoA* expressions provide evidence for microaerobic nitrification by γAOB in the suboxic zone of the Black Sea.

Whether γAOB are the main microaerobic nitrifiers or not, our results clearly show that in the Black Sea suboxic waters, microaerobic nitrification is directly coupled to anammox by providing the latter a direct local source of nitrite. Similarly, direct nitrification-anammox coupling has been suggested in the Benguela upwelling system (5), where anammox was only detected in incubations with $^{15}NH_4^+$ but not with $^{15}NO_3^-$ at one site or more, implying that nitrification rather than nitrate reduction was the source of nitrite for anammox in those cases. Currently, 30–50% of global marine nitrogen loss is estimated to occur in oceanic OMZs (9, 10) and increasing evidence has pointed to the prevalence of anammox over denitrification (5–8). If the same nitrification-anammox coupling, as observed in the Black Sea suboxic waters, also occurs in oceanic OMZs, then a substantial portion of total oceanic nitrogen loss would have come from regenerated NH_4^+ from the surface ocean, and not directly from deep-sea nitrate (SI Fig. 9).

Conclusions

A combination of microbial abundance and gene expression analyses, high-resolution chemical profiling, modeling, ^{15}N incubation experiments and statistical analyses, shows that ammonia-oxidizing crenarchaea and γAOB were both important nitrifiers in the Black Sea water column. Our data suggest that crenarchaeal ammonia-oxidizers were mainly responsible for the NO_x^- production in the lower oxic zone. This NO_x^- indirectly supported about half of the anammox activities in the suboxic zone after downward diffusion and nitrate reduction. Meanwhile, γAOB resided alongside the anammox bacteria and remained actively nitrifying in the suboxic zone, thus providing anammox bacteria with a local nitrite source. Whether the same niche-differentiation occurs in other marine environments, whether other nitrifiers remain to be found, and whether all MGI *Crenarchaeota* are capable of and do autotrophic nitrification, should be investigated. Because anammox is a major nitrogen loss in the marine environment, nitrification-anammox coupling acts as a short circuit channeling regenerated N to direct N loss, reducing the presumed direct contribution from deep-sea nitrate.

Materials and Methods

Water Sampling, Chemical Analyses, and Dark Carbon Fixation. A free-falling conductivity-temperature-depth (CTD) system (SBE 9plus; Sea-Bird Electronics, Washington, DC) equipped with an oxygen sensor (SBE 43; Sea-Bird Electronics; sampling at 24 Hz, range: 0–120%Sat, accuracy 2%Sat) was used to examine temporal variations in the physical properties of the water column. Water samples were collected by a pumpcast-CTD in high-resolution intervals, or by Go-Flo bottles on a CTD-rosette system. NH_4^+ was analyzed onboard fluorometrically (46), and NO_2^- and NO_3^- with an autoanalyzer in a shore-based laboratory. Sulfide concentration was measured onboard spectrophotometrically (47). Total dissolved Mn were determined with inductively coupled plasma and optical emission spectroscopy after filtering seawater through 0.45-μm cellulose acetate membrane filters and acidification with 250 μl of concentrated HNO_3. Particulate MnO_x were collected by *in situ* large-volume filtration (120–1,000 liters) onto glass fiber filters (GF/F; 14-cm diameter, 0.7-μm nominal pore-size). Particulate Mn was dissolved from 2-cm-diameter subsampled filter with 4 ml of 0.29 M hydroxylamine hydrochloride in 0.1 M HCl for 20 h (48) and then analyzed with flame atomic absorption spectrometry. Dark inorganic carbon fixation rates were determined as in ref. 24 with incubation time of 30–33 h.

^{15}N Incubations and Analyses. Anammox rates were measured by means of isotope-pairing (M.M.J., B.T., G.L., and M.M.M.K., unpublished results). $^{15}NO_2^-$ production was measured in the same anoxic ^{15}N incubation vials as in the anammox rate measurements, but $^{15}NO_2^-$ was analyzed as N_2 after a two-step reduction by acidified sodium iodide and then by copper at 650°C. Stable isotopic composition for N_2 was determined by gas chromatography isotopic ratio mass spectrometry. Parallel samples were incubated with allylthiourea (86 μM final conc.), and/or with 5 μM oxygen, then $^{15}NO_2^-$ production was determined.

CARD-FISH and Flow Cytometry. Sampling and processing for CARD-FISH followed previously described protocols (49, 50). The oligonucleotides probes EUB338 I-III (51, 52), Nscoc128 (53, 54), Cren554 (55), and Eury806 (56) were used to enumerate *Bacteria*, γAOB, cren- and euryarchaea respectively. Abundance of total Archaea was taken as the sum of cren- and euryarchaea. Anammox bacteria was verified by CARD-FISH with the probe BS820 (15), but strong background fluorescence precluded accurate enumeration and qPCR was used for quantification. Total microbial abundance was measured by flow cytometry (57).

Qualitative and Quantitative PCR, RT-PCR, and Phylogenetic Analyses. DNA samples were collected by large-volume *in situ* filtration onto cellulose acetate membrane filters (0.2-μm pore size), and RNA samples were collected by filtering 5–10 liters of seawater onto Sterivex filters (0.22-μm pore size; Millipore). Nucleic acids extraction, qualitative and real-time PCR and RT-PCR, and subsequent phylogenetic analyses followed established protocols (see *SI Materials and Methods*). Sequences retrieved in this study have been deposited in the GenBank under accession numbers EF414229–EF414283.

Reaction-Diffusion Modeling. Assuming steady state, fluxes of NH_4^+ and NO_x^- were calculated with a reaction-diffusion model solving the equation

$$0 = \frac{\partial}{\partial z}\left(D(z)\,\frac{\partial C}{\partial z}\right) + R,$$

where z is depth, C is NH_4^+ or NO_x^- concentration, R is production or consumption, and D is diffusivity. Rearranging the equation:

$$R = -\frac{\partial D}{\partial_z}\frac{\partial C}{\partial_z} - D(z)\,\frac{\partial^2 C}{\partial_z{}^2}.$$

Because the concentration gradients ($\partial C/\partial z$) can be computed by means of curve fitting for the concentration profiles and D can be reconstructed from *in situ* density (58), then $\partial D/\partial z$ and $\partial^2 C/\partial z^2$ can be calculated by using finite-differences formulae and subsequently R.

We thank Karsten Lettmann for model development; Daniela Franzke, Gabriele Klockgether, and Dagmar Wöbken for sampling and analytical assistance; Marc Strous and Mike Jetten (Radboud University Nijmegen, Nijmegen, The Netherlands), and Eva Spieck (University of Hamburg, Hamburg, Germany) for providing bacterial cultures; the captain and crew on the R/V *Professor Vodyanitskiy* for technical support; and two anonymous reviewers for constructive comments. P.L. was supported by the Deutsche Forschungsgemeinschaft (DFG) and Max-Planck-Gesellschaft (MPG); G.L., M.M.M.K., and R.A. were supported by the MPG; M.M.J. and B.T. were supported by the Danish National Research Foundation; and D.F.M., B.M., and C.J.S. were supported by the Eidgenössische Anstalt für Wasserversorgung, Abwasserreinigung und Gewässerschutz (EAWAG), and Eidgenössische Technische Hochschule (ETH).

1. Codispoti LA, Christensen JP (1985) *Mar Chem* 16:277–300.
2. Ward BB, Zafiriou OC (1988) *Deep-Sea Res* 35:1127–1142.
3. Lipschultz F, Wofsy SC, Ward BB, Codispoti LA, Friedrich G, Elkins JW (1990) *Deep-Sea Res* 37:1513–1541.
4. Naqvi SWA, Noronha RJ (1991) *Deep-Sea Res* 38:871–890.
5. Kuypers MMM, Lavik G, Woebken D, Schmid M, Fuchs BM, Amann R, Jorgensen BB, Jetten MSM (2005) *Proc Natl Acad Sci USA* 102:6478–6483.
6. Kuypers MMM, Lavik G, Thamdrup B (2006) in *Past and Present Marine Water Column Anoxia, NATO Science Series IV: Earth and Environmental Series*, ed Neretin LN (Springer, Dordrecht, The Netherlands), Vol 64, pp 311–336.
7. Hamersley MR, Lavik G, Woebken D, Rattray JE, Lam P, Hopmans EC, Sinninghe Damsté JS, Krüger S, Graco M, Gutiérrez D, Kuypers MMM (2007) *Limnol Oceanogr*, in press.
8. Thamdrup B, Dalsgaard T, Jensen MM, Ulloa O, Farías L, Escribano R (2006) *Limnol Oceanogr* 51:2145–2156.
9. Gruber N, Sarmiento JL (1997) *Glob Biogeochem Cycles* 11:235–266.
10. Codispoti LA, Brandes JA, Christensen JP, Devol AH, Naqvi SWA, Paerl HW, Yoshinari T (2001) *Sci Mar* 65:85–105.
11. Ward BB (2002) in *Encyclopedia of Environmental Microbiology*, ed Bitton G (Wiley, New York), pp 2144–2167.
12. Sorokin YI (2002) *The Black Sea: Ecology and Oceanography* (Backhuys Publishers, Leiden, The Netherlands).
13. Murray JW, Codispoti L, Friederich GE (1995) in *Aquatic Chemistry: Interfacial and Interspecies Processes*, eds Huang CP, O'Melia CR, Morgan JJ (Am Chem Soc, Washington, DC), pp 157–176.
14. Ward BB, Kilpatrick KA (1991) in *Black Sea Oceanography*, eds Iydar E, Murray JW (Kluwer, Dordrecht, The Netherlands), pp 111–124.
15. Kuypers MMM, Sliekers AO, Lavik G, Schmid M, Jørgensen BB, Kuenen JG, Damsté JSS, Strous M, Jetten MSM (2003) *Nature* 422:608–611.
16. Venter JC, Remington K, Heidelberg JF, Halpern AL, Rusch D, Eisen JA, Wu D, Paulsen I, Nelson KE, Nelson W, *et al.* (2004) *Science* 304:66–74.
17. Schleper C, Jurgens G, Jonuscheit M (2005) *Nat Rev Microbiol* 3:479–488.
18. Hallam SJ, Mincer TJ, Schleper C, Preston CM, Roberts K, Richardson PM, DeLong EF (2006) *PLoS Biol* 4:e95.
19. Könneke M, Bernhard AE, de la Torre JR, Walker CB, Waterbury JB, Stahl DA (2005) *Nature* 437:543–546.
20. Francis CA, Roberts KJ, Beman JM, Santoro AE, Oakley BB (2005) *Proc Natl Acad Sci USA* 102:14683–14688.
21. Karner MB, DeLong EF, Karl DM (2001) *Nature* 409:507–510.
22. Massana R, DeLong EF, Pedros-Alio C (2000) *Appl Environ Microbiol* 66:1777–1787.
23. Ingalls AE, Shah SR, Hansman RL, Aluwihare LI, Santos GM, Druffel ERM, Pearson A (2006) *Proc Natl Acad Sci USA* 103:6442–6447.
24. Herndl GJ, Reinthaler T, Teira E, van Aken H, Veth C, Pernthaler A, Pernthaler J (2005) *Appl Environ Microbiol* 71:2303–2309.
25. Wuchter C, Abbas B, Coolen MJL, Herfort L, van Bleijswijk J, Timmers P, Strous M, Teira E, Herndl GJ, Middelburg JJ, *et al.* (2006) *Proc Natl Acad Sci USA* 103:12317–12322.
26. Ward BB, Glover HE, Lipschultz F (1989) *Deep-Sea Res* 36:1031–1051.
27. Ward BB (1987) *Deep-Sea Res* 34:785–805.
28. Leininger S, Urich T, Schloter M, Schwark L, Qi J, Nicol GW, Prosser JI, Schuster SC, Schleper C (2006) *Nature* 442:806–809.
29. Bollmann A, Schmidt I, Saunders AM, Nicolaisen MH (2005) *Appl Environ Microbiol* 71:1276–1282.
30. Aoi Y, Shiramasaa Y, Masakia Y, Tsunedaa S, Hirataa A, Kitayamab A, Nagamune T (2004) *J Biotechnol* 111:111–120.
31. Aoi Y, Shiramasa Y, Tsuneda S, Hirata A, Kitayama A, Nagamune T (2002) *Water Sci Technol* 46:439–442.
32. Araki N, Yamaguchi T, Yamazaki S, Harada H (2004) *Water Sci Technol* 50:1–8.
33. Treusch AH, Leininger S, Kletzin A, Schuster SC, Klenk H-P, Schleper C (2005) *Env Microbiol* 7:1985–1995.
34. Dalsgaard T, Canfield DE, Petersen J, Thamdrup B, Acuña-González J (2003) *Nature* 422:606–608.
35. Third KA, Sliekers AO, Kuenen JG, Jetten MSM (2001) *Syst Appl Microbiol* 24:588–596.
36. Third KA, Paxman J, Schmid M, Strous M, Jetten MSM, Cord-Ruwisch R (2005) *Microb Ecol* 49:236–244.
37. Oguz T, Besiktepe S (1999) *Deep-Sea Res* 46:1733–1753.
38. Stanev EV, Staneva J, Bullister JL, Murray JW (2004) *Deep-Sea Res* 51:2137–2169.
39. Konovalov SK, Luther GW, III, Friederich GE, Nuzzio DB, Tebo BM, Murray JW, Oguz T, Glazer BT, Trouwborst RE, Clement B, *et al.* (2003) *Limnol Oceanogr* 48:2369–2376.
40. Freitag TE, Prosser JI (2003) *Appl Environ Microbiol* 69:1359–1371.
41. Mortimer RJG, Harris SJ, Krom MD, Freitag TE, Prosser JI, Barnes J, Anschutz P, Hayes PJ, Davies IM (2004) *Mar Ecol Prog Ser* 276:37–51.
42. Bodelier P, Libochant J, Blom C, Laanbroek H (1996) *Appl Environ Microbiol* 62:4100–4107.
43. Luther GWI, Sundby B, Lewis PJ, Silverburg N (1997) *Geochim Cosmochim Acta* 61:4043–4052.
44. Hulth S, Aller RC, Gilbert F (1999) *Geochim Cosmochim Acta* 63:49–66.
45. Teira E, van Aken H, Veth C, Herndl GJ (2006) *Limnol Oceanogr* 51:60–69.
46. Holmes RM, Aminot A, Kerouel R, Hooker A, Peterson BJ (1999) *Can J Fish Aqaut Sci* 56:1801–1808.
47. Cline JD (1969) *Limnol Oceanogr* 14:454–458.
48. Schippers A, Neretin LN, Lavik G, Leipe T, Pollehne F (2005) *Geochim Cosmochim Acta* 69:2241–2252.
49. Pernthaler A, Pernthaler J, Amann R (2002) *Appl Environ Microbiol* 68:3094–3101.
50. Glöckner FO, Amann R, Alreider A, Pernthaler J, Psenner R, Trebesius K, Schleifer K-H (1996) *Syst Appl Microbiol* 19:403–406.
51. Daims H, Brühl A, Amann R, Schleifer K-H, Wagner M (1999) *Syst Appl Microbiol* 22:434–444.
52. Amann R, Ludwig W, Schleifer K-H (1995) *Microbiol Rev* 59:143–169.
53. Juretschko S (2000) PhD thesis (Technische Universität, Munich, Germany).
54. Loy A, Horn M, Wagner M (2003) *Nucleic Acids Res* 31:514–516.
55. Massana R, Murray A, Preston C, DeLong E (1997) *Appl Environ Microbiol* 63:50–56.
56. Teira E, Reinthaler T, Pernthaler A, Pernthaler J, Herndl GJ (2004) *Appl Environ Microbiol* 70:4411–4414.
57. Marie D, Partensky F, Jacquet S, Vaulot D (1997) *Appl Environ Microbiol* 63:186–193.
58. Fennel K, Boss E (2003) *Limnol Oceanogr* 48:1521–1534.
59. Norton J, Alzerreca J, Suwa Y, Klotz M (2002) *Arch Microbiol* 177:139–149.